

# Systemic changes induced by autologous stem cell ovarian transplant in plasma proteome of women with impaired ovarian reserves

Anna Buigues<sup>1</sup>, Noelia Ramírez-Martin<sup>1</sup>, Jessica Martínez<sup>1</sup>, Nuria Pellicer<sup>1,2</sup>, Marcos Meseguer<sup>1,2</sup>, Antonio Pellicer<sup>1,3</sup>, Sonia Herraiz<sup>1</sup>

<sup>1</sup>IVIRMA Global Research Alliance, IVI Foundation - Instituto de Investigación Sanitaria La Fe (IIS La Fe), Valencia 46026, Spain

<sup>2</sup>IVIRMA Global Research Alliance, IVIRMA Valencia, Valencia 46015, Spain

<sup>3</sup>IVIRMA Global Research Alliance, IVIRMA Rome, Rome 00197, Italy

**Correspondence to:** Sonia Herraiz; **email:** [sonia\\_herraiz@iislafe.es](mailto:sonia_herraiz@iislafe.es)

**Keywords:** plasma proteomic profile, autologous stem cell ovarian transplantation, poor ovarian response, premature ovarian insufficiency, aging

**Received:** June 15, 2023

**Accepted:** November 10, 2023

**Published:** December 26, 2023

**Copyright:** © 2023 Buigues et al. This is an open access article distributed under the terms of the [Creative Commons Attribution License](https://creativecommons.org/licenses/by/4.0/) (CC BY 4.0), which permits unrestricted use, distribution, and reproduction in any medium, provided the original author and source are credited.

## ABSTRACT

Patients with poor ovarian response (POR) and premature ovarian insufficiency (POI) are challenging to treat, with oocyte donation remaining as the only feasible option to achieve pregnancy in some cases. The Autologous stem cell ovarian transplantation (ASCOT) technique allows follicle development, enabling pregnancies and births of healthy babies in these patients. Previous results suggest that growth factors and cytokines secreted by stem cells are partially responsible for their regenerative properties. Indeed, ASCOT beneficial effects associate with the presence of different bone marrow derived stem cell- secreted factors in plasma. Therefore, the aim of this study was to assess whether ASCOT induce any modifications in the plasma proteomic profile of patients with impaired ovarian reserves.

Discriminant analysis highlighted clear distinctions between the plasma proteome before (PRE), during stem cell mobilization and collection (APHERESIS) and three months after ASCOT (POST) in patients with POR and POI. Both the stem cell mobilization and ASCOT technique induced statistically significant modifications in the plasma composition, reversing some age-related protein expression changes. In the POR group, functional analysis revealed an enrichment in processes related to the complement cascade, immune system, and platelet degranulation, while in the POI group, enriched processes were also associated with responses to oxygen-containing compounds and growth hormones, and blood vessel maturation. In conclusion, our findings highlight the potential proteins and biological processes that may promote the follicle activation and growth observed after ASCOT. Identifying plasma proteins that regenerate aged or damaged ovaries could lead to more effective, targeted and/or preventive therapies for patients.

## INTRODUCTION

Patients with poor ovarian response (POR) or premature ovarian insufficiency (POI) are challenging to treat, with oocyte donation remaining as the only feasible

option to achieve pregnancy. Previous attempts to overcome the fertility problems of these patients have mainly been based on ovarian stimulation, and were likely unsuccessful [1] due to the lack of stimulable antral follicles remaining in the ovaries [2]. However,

emerging strategies based on platelet-rich plasma, ovarian fragmentation, and stem cell injection have reactivated residual dormant follicles to regain ovarian function [3, 4]. One of these strategies is the autologous stem cell ovarian transplantation (ASCOT), consisting of bone marrow derived stem cell (BMDSC) mobilization to peripheral blood by granulocyte-colony stimulating factor (G-CSF) treatment, collection by apheresis and infusion into the ovarian artery [5]. Our group described that the ASCOT procedure improved anti-müllerian hormone (AMH) levels and antral follicular count (AFC), as well as the number of recovered oocytes after ovarian stimulation. Ultimately, this technique enabled pregnancies and births of healthy babies in women with POR and long-lasting infertility, that were previously limited to oocyte donation [5]. Similar evidence of ovarian rescue was obtained in POI patients, in which the reactivation of ovarian function led to more efficient ovarian stimulation, and ultimately, the generation of viable embryos to transfer [6]. Interestingly, follicular growth waves and spontaneous pregnancies were observed up to six months after the ASCOT procedure [5–7], suggesting that this technique might restore folliculogenesis and produce sustained changes in the ovary through the regeneration of the ovarian stroma, as confirmed by our previous studies in mice [8].

Once mobilized, the BMDSCs circulate in peripheral blood, where they secrete paracrine growth factors that are partially responsible for their regenerative properties. Indeed, the levels of growth factors and cytokines in blood change with age. Blood from younger individuals is characterized by a myriad of growth factors and low levels of pro-inflammatory cytokines, while blood from older individuals contains fewer growth factors and an abundance of pro-inflammatory cytokines [9, 10]. Thus, the human plasma proteome may dually reflect aspects of cellular and tissue aging [11] and have an active role in the process. In this study, we aimed to assess if the ASCOT technique modifies the signature of the human plasma proteome, reveal the mechanisms underlying its beneficial effects on the ovary, and identify key regulators of ovarian aging.

## RESULTS

### Proteomic changes induced by ASCOT in patients with POR

Firstly, we assessed the proteomic changes induced by the ASCOT technique in women with POR defined according to the European Society of Human Reproduction and Embryology (ESHRE) criteria [12]. These POR patients (mean age:  $36 \pm 1$  years,  $3.0 \pm 0.0$

years of infertility) showed serum AMH levels of  $2.2 \pm 0.5$  pmol/L, and an AFC of  $2.3 \pm 0.6$  follicles at recruitment. Three months after ASCOT treatment, AMH increased to  $2.6 \pm 0.9$  pmol/L and AFC to  $5.0 \pm 1.7$  follicles. The impact of ASCOT on reproductive outcomes was previously published [5].

To elucidate whether ASCOT technique changes the plasma composition of patients with POR undergoing this reactivation technique, the proteomic profile of peripheral blood plasma was assessed before (PRE), during stem cell mobilization and collection by apheresis (APHERESIS), and three months after stem cell infusion into the ovary (POST; Supplementary Table 1). Considering the expression of the total 296 proteins quantified, the analyses of dimensionality reduction (discriminant analysis and principal component analysis) showed a clear distinction between PRE, APHERESIS, and POST samples (Figure 1A and Supplementary Figure 1A; D1: 50%, D2: 50%, PC1: 38.9%, PC2: 16.8%), confirming changes in plasma composition associated to the stem cell mobilization procedure and the ASCOT treatment.

Among the 296 proteins, 11 (3.7%) were found differentially expressed between PRE and APHERESIS conditions (Figure 1B and Supplementary Table 2), while 70 (23.6%) were differentially expressed between PRE and POST samples (Supplementary Table 3). Interestingly, eight differentially expressed proteins (DEPs) were shared between both comparisons (Supplementary Figure 1B), suggesting that the BMDSCs induced changes in plasma composition that remained for several months. Of these, the corticosteroid-binding globulin (CBG), coagulation factor XII (FA12), kininogen-1 (KNG1), along with the complement C1q B chain (C1QB), C4-A (CO4A), and component C9 (CO9) were upregulated in both the APHERESIS and POST samples, while serum albumin (ALBU) and lysosome-associated membrane glycol-protein 2 (LAMP2) were repressed.

Focusing on those effects observed three months after ASCOT, in general the heatmap analysis showed a clear separation between PRE and POST samples, with the exception of one patient in which the ASCOT technique seemed to have a lesser effect (Figure 1C). The most prominent changes after ASCOT, considering the estimated fold change, included the sushi, nidogen, and EGF like domains 1 (SNED1), plastin-2 (PLSL), vascular cell adhesion molecule 1 (VCAM1), hemoglobin subunit alpha (HBA) and peroxiredoxin-2 (PRDX2) (Supplementary Table 2).

To establish the biological relevance of the plasma changes induced by ASCOT, we queried the GO

Biological Process database and measured protein enrichment. This analysis showed none significantly associated GO biological process in APHERESIS but more than 500 pathways in POST samples (False

Discovery Rate, FDR < 0.05), being the top 30 related to protein activation, fibrin clot cascades, complement cascades, immune response, hemostasis, wound healing and exocytosis (Figure 1D).

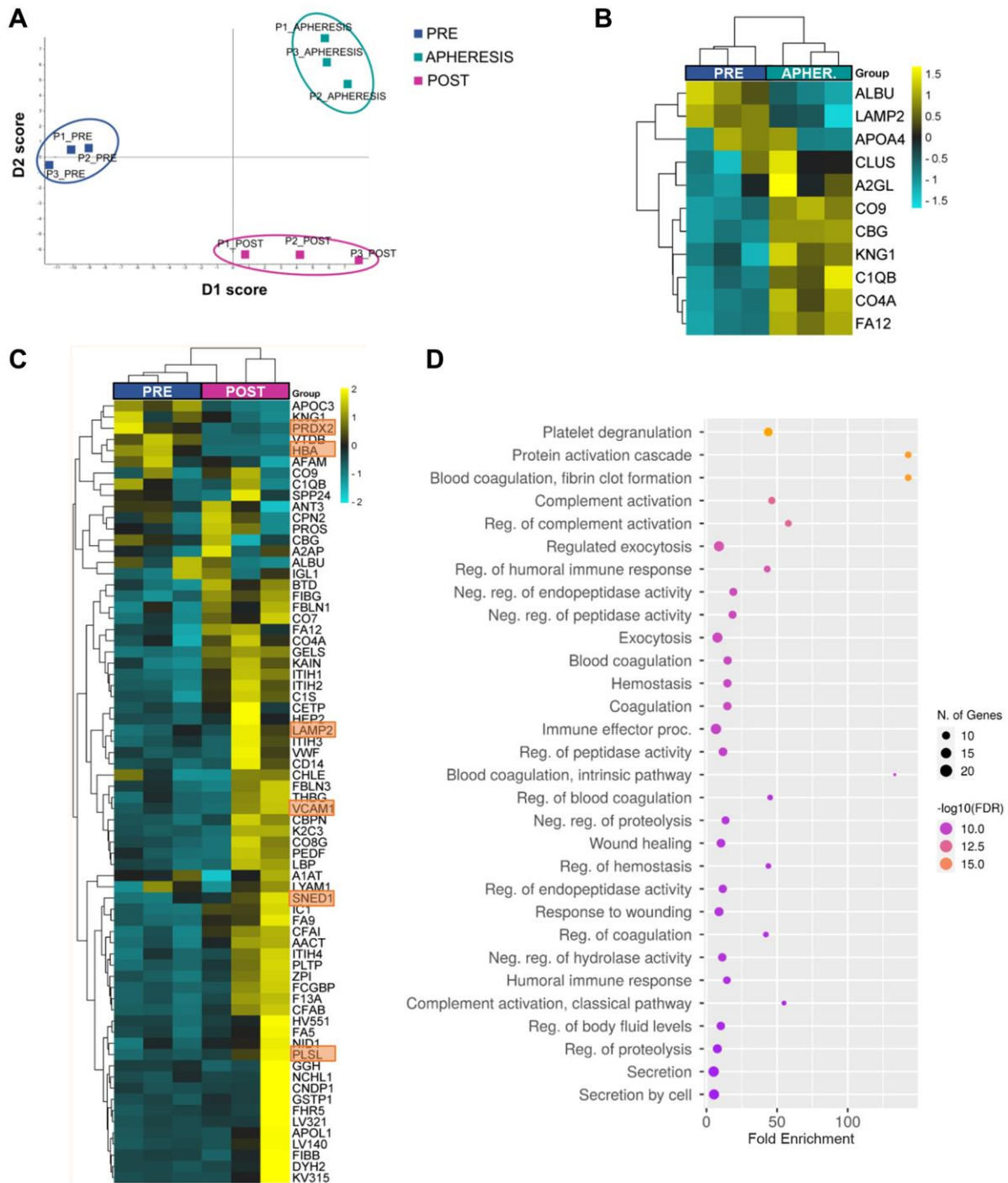


**Figure 1. Plasma proteomic changes following autologous stem cell ovarian transplantation in patients with poor ovarian response.** (A) Discriminant analysis plot considering the expression of the 296 quantified proteins, showing a clear separation between the PRE, APHERESIS, and POST samples. (B) Heatmaps depicting the hierarchical clustering of the 11 differentially expressed proteins (DEPs) between PRE and APHERESIS samples and (C) 70 DEPs between PRE and POST samples. The most prominent changes after ASCOT, considering the estimated fold change, highlighted in orange. Dot plot showing the top 30 significantly enriched (FDR < 0.05) GO biological processes three months after autologous stem cell ovarian transplantation (D). The heatmaps are color coded according to protein expression determined by SWATH™ analysis, where yellow and turquoise indicate an increase or decrease in expression, respectively.

Moreover, to understand if stem cell mobilization and infusion has the ability to restore the plasma composition, we sought to determine whether the 70 proteins whose expression significantly changed after ASCOT were linked to aging. Thus, we compared these DEPs between POST and PRE samples with proteins that change in blood with age [10, 11], and 9 were associated with aging. Among them, the expression of seven was decreased with age, but rescued with ASCOT (i.e., VCAM1, nidogen-1 (NID1), inter-alpha-trypsin inhibitor heavy chain H1 (ITI1), thyroxine-binding globulin (TBG), pigment epithelium-derived factor (PEDF), apolipoprotein L1 (APOL1), and alpha-2-antiplasmin (A2AP)), while the remaining two were overexpressed with age and repressed following treatment (i.e., Apolipoprotein C-III (APOC3) and Vitamin D-binding protein (VTDB)).

### **Proteomic changes induced by ASCOT in patients with POI**

The systemic effects of stem cell mobilization and injection in patients with POI were also assessed. This second sub-study included 6 women (mean age  $34 \pm 2$  years,  $4.0 \pm 5.4$  years of infertility) with POI according to the ESHRE criteria [13]. AMH and follicle-stimulating hormone (FSH) basal levels in these patients were  $0.09 \pm 0.08$  pmol/L and  $99.9 \pm 23.9$  IU/ml, respectively, while AFC was  $1.5 \pm 1.2$  follicles. Prior to the reactivation technique and due to the POI diagnose, these women underwent only a total of 2 IVF attempts consisting in 1 natural cycle without mature oocytes recovered and 1 cancellation due to the absence of response. Once recruited, these patients were randomized into two trial arms: 1) ASCOT group, in which the stem cells were mobilized and infused into the ovary, as described for POR women; 2) Mobilization (MOB) group, where the stem cells were mobilized but remained circulating in peripheral blood (without collection and direct ovarian infusion). The proteomic profile was assessed at the three time points previously described: at recruitment (PRE), during stem cell mobilization and collection (APHERESIS) and three months after stem cell mobilization or injection (POST). Three months after the ASCOT technique, AMH and AFC increased, and FSH decreased (Supplementary Table 4). Moreover, a total of 11 cycles of ovarian hyperstimulation were performed in these 6 patients after ASCOT (Supplementary Table 5), with a total of 9 punctured follicles, 3 collected MII oocytes and 2 embryos.

### **Systemic effects of stem cell mobilization**

A total of 431 proteins were quantified among all samples from the patients with POI (Supplementary Table 6). The analysis of dimensionality reduction

showed a clear distinction between the PRE and APHERESIS samples (Figure 2A; D1: 50%, D2: 50%), characterized by the presence of 14 DEPs (3.2% of the total; Figure 2B). Specifically, both the complement C1q subcomponent subunit A (C1QA) and complement C1r subcomponent (C1R) exhibited the highest change for the estimated fold change (Supplementary Table 7). Accordingly, functional analysis highlighted significant enrichment of pathways related to complement cascades and immune response (Figure 2C). Moreover, when the link of these proteomic changes with aging was evaluated, we found three proteins that were upregulated in APHERESIS whose plasma levels decrease with aging (i.e., complement C1q subcomponent subunit C (C1QC), lysozyme C (LYSC), and L-selectin (LYAM1)), and one downregulated protein (i.e., C-reactive protein (CRP)) whose expression rises with age [11].

Interestingly, the POST samples showed a clearly different proteomic pattern in each study arm (Figure 2A), highlighting an effect of stem cell infusion. Therefore, each arm was considered independently to determine the systemic effects of stem cell mobilization and injection (with respect to their corresponding PRE groups).

### **Specific effects in the mobilization arm**

Within the mobilization arm, we identified 24 DEPs between PRE and POST groups (5.6% of the total; Figure 3A; Supplementary Table 8), suggesting that stem cell mobilization, alone, can elicit systemic changes that persist over time. Next, functional analysis revealed that these changes were associated with responses related to the immune system, oxygen-containing compounds, wounding, and growth hormones, in addition to cell adhesion, platelet degranulation, and blood vessel maturation (Figure 3B). Notably, increased plasma levels of two DEPs (i.e., 72 kDa type IV collagenase (MMP2) and fructose-bisphosphate aldolase C (ALDOC)) which were described to decrease with age [11].

### **Specific effects of stem cell injection (ASCOT arm)**

To determine how stem cell injection affected plasma proteome, we compared POST samples of patients included in the ASCOT arm with their corresponding PRE samples.

These samples were also clearly differentiated (Figure 2A), although only 11 DEPs were identified (Figure 3C, Supplementary Table 9), and no significantly associated GO Biological Processes were found. Nevertheless, amidst these DEPs, we found the di-N-acetylchitobiase (DIAC) whose plasma levels increase with aging [11] and was downregulated after ASCOT.

Additionally, the comparison between POST samples from both study arms identified only one shared DEP (Figure 3D), suggesting that those proteomic changes in peripheral plasma after the technique depend not only on stem cell mobilization, but also on ovarian injection. Indeed, 16 DEPs (Supplementary

Figure 2A; Supplementary Table 10) related to platelet degranulation, catabolic processes, immune response, blood coagulation, proteolysis, complement cascades, and plasma lipoprotein oxidation (Supplementary Figure 2B), were found between POST samples of both study arms.

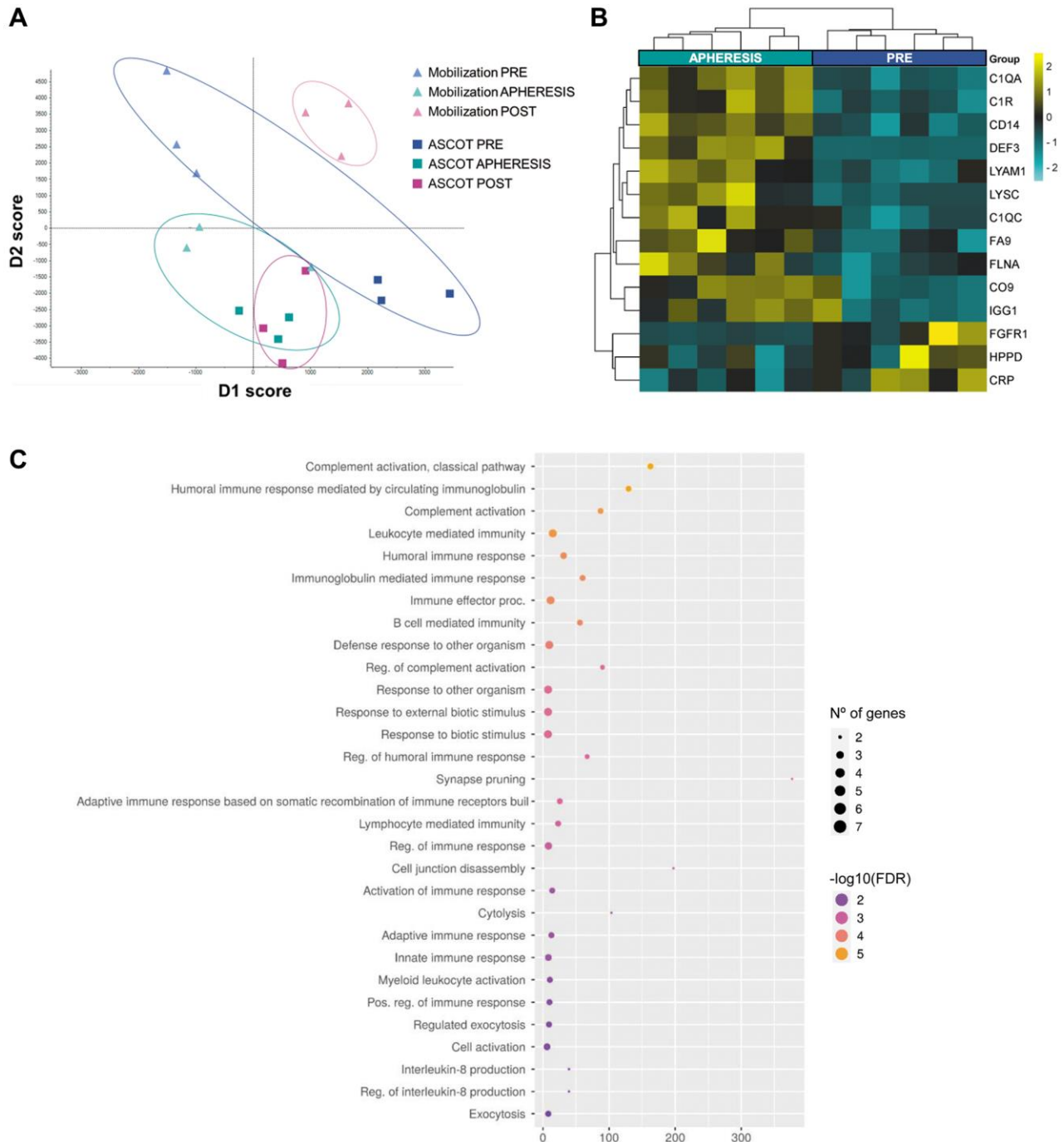


**Figure 2. Plasma proteomic changes following stem cell mobilization in patients with premature ovarian insufficiency.** (A) Discriminant analysis plot considering all PRE and all APHERESIS samples together. ASCOT, autologous stem cell ovarian transplantation. Heatmap depicting the hierarchical clustering of the 14 differentially expressed proteins between the PRE and APHERESIS samples (B), and dot plot showing the corresponding top 30 significantly enriched (FDR < 0.05) GO biological processes (C). The heatmap is color coded according to protein expression determined by SWATH™ analysis, where yellow and turquoise indicate an increase or decrease in expression, respectively.

### Comparative assessment of plasma proteomic changes associated to the ASCOT technique in patients with POR and POI

Finally, we compared the DEPs between patients with POR and POI to assess if modifications of proteomic profiles after stem cell mobilization and infusion change according to diagnosis.

We found that only one protein (CO9) was commonly upregulated between the APHERESIS samples of patients with POR and POI after stem cell mobilization (Figure 4A).

The stem cell infusion procedure also induced different systemic changes between patients with POR and POI patients from the ASCOT arm (with

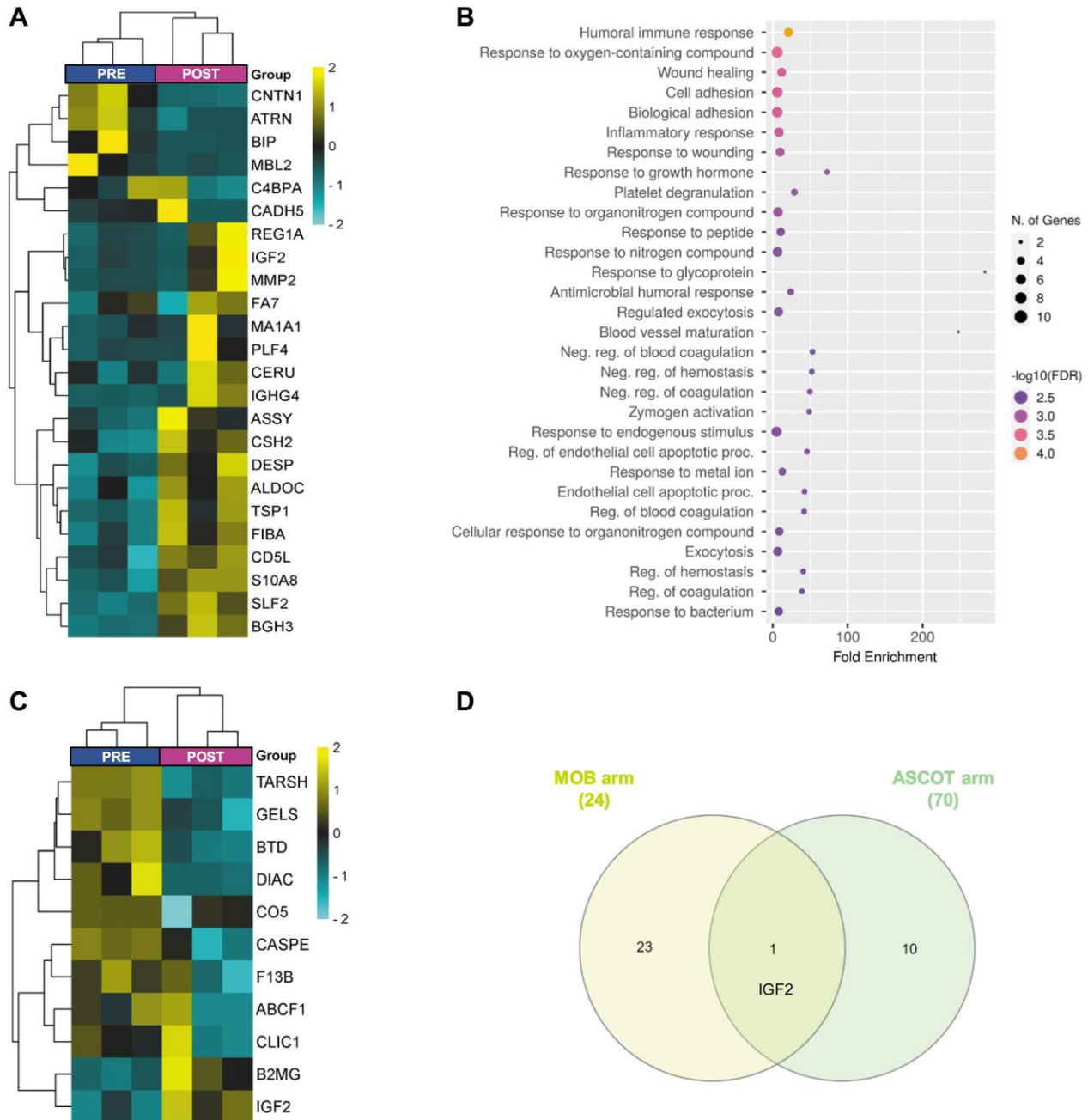
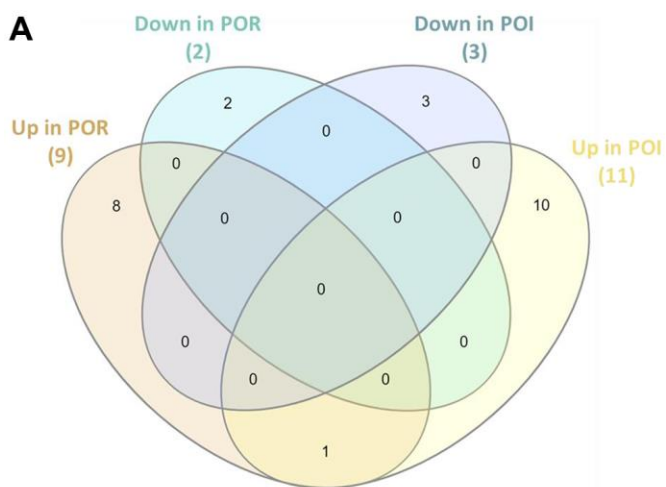


**Figure 3. Plasma proteomic changes three months after stem cell mobilization/injection in patients with premature ovarian insufficiency.** Heatmap depicting the hierarchical clustering of the 24 differentially expressed proteins (DEPs) between PRE and POST samples in the mobilization arm (A), and dot plot showing the corresponding top 30 significantly enriched (FDR < 0.05) GO biological processes (B). (C) Heatmap depicting the hierarchical clustering of the 11 DEPs between PRE and POST samples in the ASCOT arm. (D) Venn diagram highlighting the shared DEPs between POST samples of both study arms. The heatmaps are color coded according to protein expression determined by SWATH™ analysis, where yellow and turquoise indicate an increase or decrease in expression, respectively.

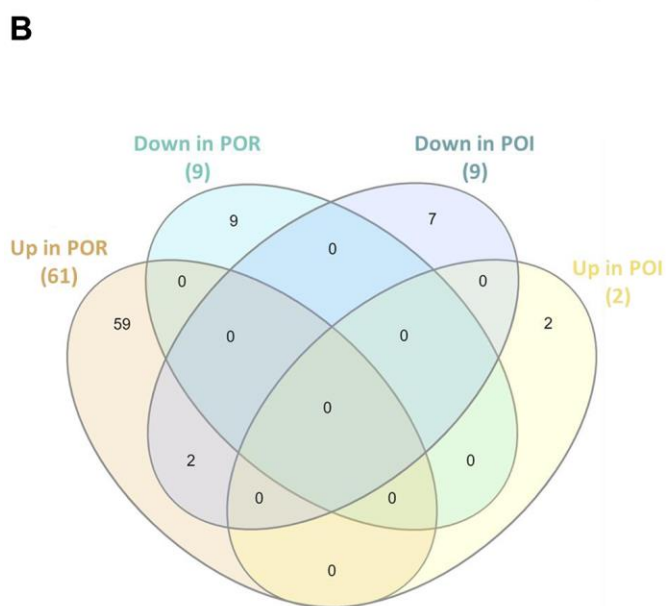
cell infusion), as shown in Figure 4B. In fact, the only two shared DEPs following stem cell injection were biotinidase (BTD) and gelsolin (GELS), which were upregulated in POR and downregulated in POI patients.

## DISCUSSION

Blood is considered a sensitive marker for functional aging, with an active role in this process. In fact, several studies have shown that the soluble factors present in



Up in POR	Down in POR	Up in POI	Down in POI
A2GL	ALBU	C1QA	CRP
KNG1	LAMP2	C1R	HPPD
C1QB		LYAM1	FGFR1
CLUS		DEF3	
<b>CO9</b>		FA9	
CBG		CD14	
APOA4		<b>CO9</b>	
CO4A		LYSC	
FA12		C1QC	
		FLNA	
		IGG1	



Up in POR	Down in POR	Up in POI	Down in POI
SNED1	GSTP1	K2C3	B2MG
PLSL	FA9	ALBU	IGF2
VCAM1	CBPN	AFAM	
CETP	LYAM1	APOC3	
LBP	LV321	VTDB	
NID1	FIBB	SPP24	
CD14	THBG	LAMP2	
FIBG	ITIH3	PRDX2	
IGL1	PEDF	HBA	
NCHL1	FHR5		
CFAB	KNG1		
ITIH1	<b>BTD</b>		
VWF	PLTP		
CO8G	CBG		
CO7	ZPI		
F13A	CPN2		
C1QB	CNDP1		
FA5	ITIH4		
ITIH2	DYH2		
HEP2	IC1		
AACT	LV140		
FA12	HV551		
KAIN	A1AT		
<b>GELS</b>	CHLE		
C1S	ANT3		
FBLN3	APOL1		
CO4A	A2AP		
CO9	GGH		
CFAI	FCGBP		
FBLN1	KV315		
PROS			

**Figure 4. Comparative assessment of the proteomic effects of stem cell mobilization and injection in patients with poor ovarian response (POR) and premature ovarian insufficiency (POI).** (A) Venn diagram (left) and protein name (right) of the differentially expressed proteins in Apheresis samples of patients with POR and POI (both study arms), showing the relationships between the type of protein regulation (up/down). (B) Venn diagram (left) and protein name (right) of the differentially expressed proteins three months after autologous stem cell ovarian transplantation (ASCOT) in patients with POR and patients with POI from the ASCOT arm, showing the relationships between the type of protein regulation (up/down). The total number of significant differentially expressed proteins in each category is represented in brackets.

blood from younger individuals can reverse some aspects and clinical signs of aging [9, 14–16]. Based on these findings, along with the long-term fertility restoration induced by ASCOT in women with POR/POI and our murine models of ovarian damage, we aimed to evaluate the plasma proteome modifications induced by ASCOT, with special interest in those proteins with potential ovarian regenerative properties.

Our functional analyses suggested that, overall, the ASCOT technique affects biological processes related to platelet activation and degranulation, the immune system and the complement cascade. Platelet release of growth factors becomes less efficient with age [10], and alterations in immune responses have been proposed as major causes of ovarian aging [17]. Likewise, complement cascades are related to folliculogenesis, oocyte maturation, and ovarian aging [18, 19]. In this context, our results suggest that the promotion of follicle growth and ovulation observed after ASCOT [5] may be elicited by the proteomic changes of the complement system.

In the POR cohort, almost all the DEPs in the APHERESIS samples were also detected in the POST samples, suggesting that BMDSCs induced proteomic changes in plasma composition that remain over time and that could underlie the second wave of follicular growth previously observed 3 months after ASCOT, and numerous spontaneous pregnancies reported more than 6 months after the procedure [5]. Of the DEPs from the POST samples, the most prominent change was observed for SNED1, an extracellular matrix (ECM) protein. Notably, the ECM is altered with ovarian aging [20, 21], and affects follicle development, oocyte quality, fibrosis, and vascularization [22–26]. In fact, a restoration of ovulation and an extension of the reproductive lifespan of female mice was achieved by reverting the ovarian fibrosis occurring with aging [27]. Therefore, the promotion of follicle growth observed after ASCOT [5] could be related to changes in the ECM, as our previous studies using murine models suggested [8], and SNED1 might play a key role in these effects within the ovarian niche. Moreover, the ASCOT procedure increased proteins whose levels are reduced with aging (such as VCAM1, NID1, ITIH1, THBG, PEDF, APOL1, and A2AP), and repressed others that increase with age (i.e., APOC3 and VTDB) [10, 11]. These findings supported that ASCOT may partially reverse some age-related proteomic changes in plasma, providing factors with potential regenerative properties in the ovaries. It is important to note that the levels of VCAM1, ITIH1, and APOL1 are reduced in the wave of plasma protein changes that occurs at the age of 34 [11], when ovarian aging begins [28].

VCAM1 plays a crucial role in age-related ovarian vascular alterations, such as increased oxidative stress, vascular fibrosis, and endothelial barrier impairment [17, 29, 30]. Thus, the ASCOT technique might optimize ovarian function by reverting the decline of the aforementioned proteins, which are likely involved in ovarian aging. However, further investigation of the proteins we identified is warranted to determine whether they truly play a role in the ovarian regenerative effects observed after ASCOT in women with POR.

In patients with POI, stem cell mobilization also modified the plasma proteomic profile, however the DEPs in APHERESIS samples differed from those observed in patients with POR, with only one common upregulated protein. This finding suggests that although mobilization may affect similar biological processes, the downstream effects depend on the diagnosis of the patient. This finding is consistent with previous data showing differences in apheresis composition with menstrual cycle phase and hormone levels [31]. In fact, although POI and POR patients can be mixed up, they represent different clinical entities, showing differences in menses cyclicity and sexual hormone profile.

Our study revealed that the G-CSF mobilization treatment, *per se*, induced changes in the plasma proteomic composition still detectable 3 months after treatment, that might be linked to follicular growth observed in patients of the mobilization arm [6, 7]. This is consistent with tissue regeneration induced by G-CSF treatment, due to the ability of BMDSCs to migrate and engraft in damaged tissues and organs [32–35]. These effects of mobilization in women with POI would be related to the immune system and platelet degranulation, responses to oxygen-containing compounds and growth hormones, and blood vessel maturation, which are all processes associated with the oocyte's bioenergetics and quality [36], folliculogenesis and ovulation [37, 38]. Among those systemic changes induced by G-CSF mobilization that remain detectable for a few months, we observed an up-regulation of MMP2 and ALDOC, whose levels are described to decrease in plasma with aging [11]. MMP2 degrades ECM proteins, and as such, is involved in diverse functions (e.g., vascular remodeling, angiogenesis, tissue repair, and inflammation). Further, the ovarian expression of MMP2 decreased with age [21]. Based on the ovarian niche regeneration and microvessel formation induced by the intravenous administration of BMDSCs in murine models of POI [8], MMP2 appears to be a key player in the beneficial effects of these stem cells. Likewise, ALDOC stimulates follicle activation [39] and, therefore, might be involved in the late wave of follicle growth observed in patients with POI six

months after stem cell mobilization [6, 7] – which aligns with the 5–6 month period required for a human primordial follicle to reach the preovulatory stage [40].

On the other hand, direct BMDSCs infusion into the ovary also produced non-transient changes in the plasma proteomic profile of women with POI, however, there were fewer and diverse DEPs from those caused by G-CSF mobilization alone, highlighting an effect of stem cell injection. Interestingly, only insulin-like growth factor II (IGF2) was differentially expressed in POST samples of both study arms. The levels of IGF2 have been reported to decrease in serum and oocytes with aging, and thus, its supplementation could potentially enhance oocyte competence [41, 42]. Besides IGF2, another ten DEPs were found in POST ASCOT samples, including F13B and TARSH, which are dysregulated in women with PCOS [43, 44], and ABCF1, which regulates innate immune responses and DNA repair [45].

In conclusion, our results showed that G-CSF mobilization and our ASCOT technique elicits proteomic changes in peripheral blood plasma composition in both POR and POI women that remain for few months. Specifically, stem cell mobilization and infusion reversed age-related proteomic changes, particularly those occurring in the wave of changes that occurs at the age of 34, when ovarian aging begins [10, 11]. These proteins would be involved in the activation and promotion of follicle growth observed following the ASCOT technique, and could be key regulators of ovarian aging. We aimed to investigate those blood-borne changes induced by the ASCOT technique in these patients, who may already present an altered plasmatic profile, to explain the ovarian effects detected months after ASCOT [5]. However, further investigation including a reference group of age-matched fertile women will be required to assess how the ovarian diagnose affects plasma composition and if the technique restores proteomic condition. Moreover, considering the small sample size used in this study, further experimental studies will also be needed to determine the extent of their regenerative effects within the ovaries, and their direct implications in ovarian aging. Identifying plasma proteins that regenerate aged or damaged ovaries could lead to more effective, targeted and/or preventive therapies for affected patients.

## METHODS

### Ethical approval

All study procedures were approved by the Institutional Review Board of the Hospital Universitario y

Politécnico La Fe, in Valencia, Spain (2014/0147 and 2017/0251) and in accordance with the principles expressed in the Declaration of Helsinki.

### Study design

Blood samples from women with POR and POI, included in our previous ASCOT pilot studies (NCT02240342 and NCT03535480), were employed in this study.

Patients with POR ( $N = 3$ ), defined according to the European Society of Human Reproduction and Embryology (ESHRE) criteria [12], were treated with G-CSF (10 mg/kg/day, subcutaneously) during 5 days to mobilize the stem cells from the bone marrow to peripheral blood. On day fifth, the BMDSCs were collected by apheresis, and infused into the ovarian artery by intra-arterial catheterization, as previously described [5]. Meanwhile, as described before, six POI patients according to the ESHRE criteria [13] were divided into two trial arms: (1) ASCOT, in which the stem cells were mobilized and infused into the ovary, as described for POR women; (2) Mobilization (MOB), in which the mobilized stem cells remained circulating in peripheral blood without local transplant in the ovary. Plasma samples were collected before (PRE), during (APHERESIS) and three months after stem cell mobilization and injection (POST), assessing the proteomic profile of each time point by the high throughput quantitative SWATH™ technique.

### Sample collection and plasma isolation

The peripheral blood was collected in BD Vacutainer® EDTAK2 tubes (BD Diagnostics, NJ, USA) prior to, and three months after, stem cell mobilization (PRE and POST samples, respectively). An aliquot of the apheresis of each patient was also collected in EDTA tubes. Plasma samples were isolated through centrifugation (for 10 min at 4°C), and stored at –80°C until further use. Plasma samples from three patients with POR and six patients with POI (three in each study arm) were then analyzed by proteomic techniques.

### Proteomic assessment of plasma samples by LC-MS/MS and SWATH™ analysis

A quantitative proteomic approach using SWATH™ was applied to analyze the proteomic profiles of plasma from PRE, APHERESIS, and POST samples.

To prepare the samples for proteomic analysis, 150 µL of each plasma sample was centrifuged at 15,000 × g for 15 min at 5°C, to separate the lipoproteins present in

the circulating blood. Samples were then pooled to build a library, as described in the Supplementary Materials.

Once the library was generated, the PRE, APHERESIS, and POST samples from the POR and POI patients were analyzed individually. The proteins were extracted from each sample, quantified, and digested as described in the Supplementary Materials. Digested peptide mixtures (5  $\mu$ L) were loaded onto NanoLC Columns (3  $\mu$  C18-CL, 75  $\mu$ m  $\times$  15 cm; Eksigent Technologies, CA, USA) and desalted with 0.1% trifluoroacetic acid at 2  $\mu$ L/min during 10 min. Analytical columns (LC Column, 3  $\mu$  C18-CL, 75  $\mu$ m  $\times$  12 cm; Nikkyo Japan) were equilibrated in 5% acetonitrile with 0.1% formic acid, before eluting peptides with a linear gradient of 5–35% acetonitrile solution in 0.1% formic acid for 120 min (flow rate: 300 nL/min). Peptides were analyzed in a mass spectrometer nanoESI qTOF (5600 TripleTOF; AB Sciex, MA, USA) operating in SWATH mode, in which a 0.050-s TOF MS scan from 350–1250 m/z was performed, followed by 0.080-s product ion scans from 350–1250 m/z on the 32 defined windows (3.05 sec/cycle). Thirty-seven SWATH windows were used, with 15 Da window widths, from 450 to 1000 Da. The individual samples were randomized in blocks and the total ions were counted. The resulting wiff files were analyzed using Peak View 2.1 with the previously generated “Pan Serum Library”. The processing settings used for the peptide selection are indicated in the Supplementary Materials. After peptide detection, the retention times were realigned using the high-confidence peptides from the library, and peptides were re-analyzed with a 10 min XIC extraction window. Proteins were quantified employing Marker View (Sciex, MA, USA), and the computed protein areas were normalized by the total sum of the areas of all the quantified proteins.

### Statistical analysis

Exploratory multidimensional analysis of proteomic data was performed using principal component analysis and discriminant analysis to reduce dimensionality and explore the results of SWATH™ assessment. To this end, R software [46] was employed. Then, a penalized linear regression ElasticNet model was applied using R, and the glmnet library was employed to DEPs among PRE and APHERESIS samples, and PRE and POST samples, in patients with POR and POI. Specifically, after a logarithmic transformation of the SWATH quantified protein areas, the train function of the Caret package was employed to obtain the parameters needed for ElasticNet penalized linear regression.

Finally, to determine the biological processes affected by BMDSCs mobilization and infusion into the ovary, a Gene Ontology Enrichment Analysis for the differentially expressed proteins was performed using the ShinyGO web-tool (version 0.741). GO Biological Processes with a FDR < 0.05 were considered significantly enriched, and the top thirty were selected and represented in dotplot charts.

### AUTHOR CONTRIBUTIONS

AB contributed to study conception and design, performed data analysis and data interpretation, created the figures and wrote the article; NRM participated in data interpretation and reviewed the article; JM participated in data acquisition and analysis; NP participated in data acquisition/analysis and drafting; MM contributed to funding acquisition and revised the article. AP contributed to funding acquisition, study conception and design and revised the article. SH contributed to study conception and design, data interpretation, writing, review and editing. The final article and order of authorship has been approved by all authors.

### ACKNOWLEDGMENTS

The authors acknowledge the technical assistance from the Proteomics Facility of the SCSIE University of Valencia, Valencia, Spain (member of the PRB2-ISCIII ProteoRed Proteomics Platform) for the proteomic analysis of the plasma samples used in this study.

### CONFLICTS OF INTEREST

The authors declare no conflicts of interest related to this study.

### ETHICAL STATEMENT AND CONSENT

All study procedures were approved by the Institutional Review Board of the Hospital Universitario y Politécnico La Fe, in Valencia, Spain (2014/0147 and 2017/0251) and in accordance with the principles expressed in the Declaration of Helsinki. Written informed consent to collect and analyze plasma and cell samples was obtained at recruitment stage.

### FUNDING

This work was supported by grants from the Regional Valencian Ministry of Innovation, Universities, Science and Digital Society (CIPROM/2021/058 (AP)); Spanish Ministry of Science, Innovation and Universities (FPU19/0496 (NRM)); Instituto de Salud Carlos III (ISCIII; PI21/00170 (SH) and CD20/00116 (AB) co-funded by the European Union, CP19/00141 (SH)

co-funded by the European Social Fund (ESF) “Investing in your future”).

## REFERENCES

1. Kyrou D, Kolibianakis EM, Venetis CA, Papanikolaou EG, Bontis J, Tarlatzis BC. How to improve the probability of pregnancy in poor responders undergoing in vitro fertilization: a systematic review and meta-analysis. *Fertil Steril*. 2009; 91:749–66. <https://doi.org/10.1016/j.fertnstert.2007.12.077> PMID:[18639875](https://pubmed.ncbi.nlm.nih.gov/18639875/)
2. Pellicer A, Ardiles G, Neuspiller F, Remohí J, Simón C, Bonilla-Musoles F. Evaluation of the ovarian reserve in young low responders with normal basal levels of follicle-stimulating hormone using three-dimensional ultrasonography. *Fertil Steril*. 1998; 70:671–5. [https://doi.org/10.1016/s0015-0282\(98\)00268-4](https://doi.org/10.1016/s0015-0282(98)00268-4) PMID:[9797096](https://pubmed.ncbi.nlm.nih.gov/9797096/)
3. Li J, Kawamura K, Cheng Y, Liu S, Klein C, Liu S, Duan EK, Hsueh AJ. Activation of dormant ovarian follicles to generate mature eggs. *Proc Natl Acad Sci U S A*. 2010; 107:10280–4. <https://doi.org/10.1073/pnas.1001198107> PMID:[20479243](https://pubmed.ncbi.nlm.nih.gov/20479243/)
4. Pellicer N, Cozzolino M, Diaz-García C, Galliano D, Cobo A, Pellicer A, Herraiz S. Ovarian rescue in women with premature ovarian insufficiency: facts and fiction. *Reprod Biomed Online*. 2023; 46:543–65. <https://doi.org/10.1016/j.rbmo.2022.12.011> PMID:[36710157](https://pubmed.ncbi.nlm.nih.gov/36710157/)
5. Herraiz S, Romeu M, Buigues A, Martínez S, Díaz-García C, Gómez-Seguí I, Martínez J, Pellicer N, Pellicer A. Autologous stem cell ovarian transplantation to increase reproductive potential in patients who are poor responders. *Fertil Steril*. 2018; 110:496–505.e1. <https://doi.org/10.1016/j.fertnstert.2018.04.025> PMID:[29960701](https://pubmed.ncbi.nlm.nih.gov/29960701/)
6. Pellicer de Castellví N. Trasplante autólogo de médula ósea en ovario en mujeres con baja reserva ovárica y fallo ovárico precoz, para rejuvenecimiento del nicho ovárico y favorecimiento del desarrollo folicular. Universitat de València, Department of pediatrics, obstetrics and gynaecology. 2020.
7. Pellicer N, Herraiz S, Romeu M, Martínez S, Buigues A, Gómez-Seguí I, Martínez J, Pellicer A. Bone Marrow derived stem cells restore ovarian function and fertility in premature ovarian insufficiency women. Interim report of a randomized trial: mobilization versus ovarian injection. 36th Virtual Annual Meeting of the European Society of Human Reproduction and Embryology. *Hum Reprod*. 2020 (Suppl 1); 35:i38–9.
8. Herraiz S, Buigues A, Díaz-García C, Romeu M, Martínez S, Gómez-Seguí I, Simón C, Hsueh AJ, Pellicer A. Fertility rescue and ovarian follicle growth promotion by bone marrow stem cell infusion. *Fertil Steril*. 2018; 109:908–18.e2. <https://doi.org/10.1016/j.fertnstert.2018.01.004> PMID:[29576341](https://pubmed.ncbi.nlm.nih.gov/29576341/)
9. Villeda SA, Plambeck KE, Middeldorp J, Castellano JM, Mosher KI, Luo J, Smith LK, Bieri G, Lin K, Berdnik D, Wabl R, Udeochu J, Wheatley EG, et al. Young blood reverses age-related impairments in cognitive function and synaptic plasticity in mice. *Nat Med*. 2014; 20:659–63. <https://doi.org/10.1038/nm.3569> PMID:[24793238](https://pubmed.ncbi.nlm.nih.gov/24793238/)
10. Castellano JM, Mosher KI, Abbey RJ, McBride AA, James ML, Berdnik D, Shen JC, Zou B, Xie XS, Tingle M, Hinkson IV, Angst MS, Wyss-Coray T. Human umbilical cord plasma proteins revitalize hippocampal function in aged mice. *Nature*. 2017; 544:488–92. <https://doi.org/10.1038/nature22067> PMID:[28424512](https://pubmed.ncbi.nlm.nih.gov/28424512/)
11. Lehallier B, Gate D, Schaum N, Nanasi T, Lee SE, Yousef H, Moran Losada P, Berdnik D, Keller A, Verghese J, Sathyan S, Franceschi C, Milman S, et al. Undulating changes in human plasma proteome profiles across the lifespan. *Nat Med*. 2019; 25:1843–50. <https://doi.org/10.1038/s41591-019-0673-2> PMID:[31806903](https://pubmed.ncbi.nlm.nih.gov/31806903/)
12. Ferraretti AP, La Marca A, Fauser BC, Tarlatzis B, Nargund G, Gianaroli L, and ESHRE working group on Poor Ovarian Response Definition. ESHRE consensus on the definition of 'poor response' to ovarian stimulation for in vitro fertilization: the Bologna criteria. *Hum Reprod*. 2011; 26:1616–24. <https://doi.org/10.1093/humrep/der092> PMID:[21505041](https://pubmed.ncbi.nlm.nih.gov/21505041/)
13. Webber L, Davies M, Anderson R, Bartlett J, Braat D, Cartwright B, Cifkova R, de Muinck Keizer-Schrama S, Hogervorst E, Janse F, Liao L, Vlaisavljevic V, Zillikens C, Vermeulen N, and European Society for Human Reproduction and Embryology (ESHRE) Guideline Group on POI. ESHRE Guideline: management of women with premature ovarian insufficiency. *Hum Reprod*. 2016; 31:926–37. <https://doi.org/10.1093/humrep/dew027> PMID:[27008889](https://pubmed.ncbi.nlm.nih.gov/27008889/)
14. Baht GS, Silkstone D, Vi L, Nadesan P, Amani Y, Whetstone H, Wei Q, Alman BA. Exposure to a youthful circulation rejuvenates bone repair through modulation of  $\beta$ -catenin. *Nat Commun*. 2015; 6:7131. <https://doi.org/10.1038/ncomms8131>

- PMID:[25988592](https://pubmed.ncbi.nlm.nih.gov/25988592/)
15. Katsimpardi L, Litterman NK, Schein PA, Miller CM, Loffredo FS, Wojtkiewicz GR, Chen JW, Lee RT, Wagers AJ, Rubin LL. Vascular and neurogenic rejuvenation of the aging mouse brain by young systemic factors. *Science*. 2014; 344:630–4.  
<https://doi.org/10.1126/science.1251141>  
PMID:[24797482](https://pubmed.ncbi.nlm.nih.gov/24797482/)
  16. Loffredo FS, Steinhauser ML, Jay SM, Gannon J, Pancoast JR, Yalamanchi P, Sinha M, Dall'Osso C, Khong D, Shadrach JL, Miller CM, Singer BS, Stewart A, et al. Growth differentiation factor 11 is a circulating factor that reverses age-related cardiac hypertrophy. *Cell*. 2013; 153:828–39.  
<https://doi.org/10.1016/j.cell.2013.04.015>  
PMID:[23663781](https://pubmed.ncbi.nlm.nih.gov/23663781/)
  17. Ma L, Lu H, Chen R, Wu M, Jin Y, Zhang J, Wang S. Identification of Key Genes and Potential New Biomarkers for Ovarian Aging: A Study Based on RNA-Sequencing Data. *Front Genet*. 2020; 11:590660.  
<https://doi.org/10.3389/fgene.2020.590660>  
PMID:[33304387](https://pubmed.ncbi.nlm.nih.gov/33304387/)
  18. Nilsson EE, Savenkova MI, Schindler R, Zhang B, Schadt EE, Skinner MK. Gene bionetwork analysis of ovarian primordial follicle development. *PLoS One*. 2010; 5:e11637.  
<https://doi.org/10.1371/journal.pone.0011637>  
PMID:[20661288](https://pubmed.ncbi.nlm.nih.gov/20661288/)
  19. Yoo SW, Bolbot T, Koulova A, Sneeringer R, Humm K, Dagon Y, Usheva A. Complement factors are secreted in human follicular fluid by granulosa cells and are possible oocyte maturation factors. *J Obstet Gynaecol Res*. 2013; 39:522–7.  
<https://doi.org/10.1111/j.1447-0756.2012.01985.x>  
PMID:[22925265](https://pubmed.ncbi.nlm.nih.gov/22925265/)
  20. Briley SM, Jasti S, McCracken JM, Hornick JE, Fegley B, Pritchard MT, Duncan FE. Reproductive age-associated fibrosis in the stroma of the mammalian ovary. *Reproduction*. 2016; 152:245–60.  
<https://doi.org/10.1530/REP-16-0129>  
PMID:[27491879](https://pubmed.ncbi.nlm.nih.gov/27491879/)
  21. Pennarossa G, De Iorio T, Gandolfi F, Brevini TAL. Impact of Aging on the Ovarian Extracellular Matrix and Derived 3D Scaffolds. *Nanomaterials (Basel)*. 2022; 12:345.  
<https://doi.org/10.3390/nano12030345>  
PMID:[35159690](https://pubmed.ncbi.nlm.nih.gov/35159690/)
  22. Ouni E, Bouzin C, Dolmans MM, Marbaix E, Pyr Dit Ruys S, Vertommen D, Amorim CA. Spatiotemporal changes in mechanical matrix components of the human ovary from prepuberty to menopause. *Hum Reprod*. 2020; 35:1391–410.  
<https://doi.org/10.1093/humrep/deaa100>  
PMID:[32539154](https://pubmed.ncbi.nlm.nih.gov/32539154/)
  23. Wood CD, Vijayvergia M, Miller FH, Carroll T, Fasanati C, Shea LD, Brinson LC, Woodruff TK. Multi-modal magnetic resonance elastography for noninvasive assessment of ovarian tissue rigidity in vivo. *Acta Biomater*. 2015; 13:295–300.  
<https://doi.org/10.1016/j.actbio.2014.11.022>  
PMID:[25463483](https://pubmed.ncbi.nlm.nih.gov/25463483/)
  24. Bonnans C, Chou J, Werb Z. Remodelling the extracellular matrix in development and disease. *Nat Rev Mol Cell Biol*. 2014; 15:786–801.  
<https://doi.org/10.1038/nrm3904>  
PMID:[25415508](https://pubmed.ncbi.nlm.nih.gov/25415508/)
  25. Bateman JF, Boot-Handford RP, Lamandé SR. Genetic diseases of connective tissues: cellular and extracellular effects of ECM mutations. *Nat Rev Genet*. 2009; 10:173–83.  
<https://doi.org/10.1038/nrg2520>  
PMID:[19204719](https://pubmed.ncbi.nlm.nih.gov/19204719/)
  26. Pickup MW, Mouw JK, Weaver VM. The extracellular matrix modulates the hallmarks of cancer. *EMBO Rep*. 2014; 15:1243–53.  
<https://doi.org/10.15252/embr.201439246>  
PMID:[25381661](https://pubmed.ncbi.nlm.nih.gov/25381661/)
  27. Umehara T, Winstanley YE, Andreas E, Morimoto A, Williams EJ, Smith KM, Carroll J, Febbraio MA, Shimada M, Russell DL, Robker RL. Female reproductive life span is extended by targeted removal of fibrotic collagen from the mouse ovary. *Sci Adv*. 2022; 8:eabn4564.  
<https://doi.org/10.1126/sciadv.abn4564>  
PMID:[35714185](https://pubmed.ncbi.nlm.nih.gov/35714185/)
  28. Broekmans FJ, Soules MR, Fauser BC. Ovarian aging: mechanisms and clinical consequences. *Endocr Rev*. 2009; 30:465–93.  
<https://doi.org/10.1210/er.2009-0006>  
PMID:[19589949](https://pubmed.ncbi.nlm.nih.gov/19589949/)
  29. Kleefeldt F, Bömmel H, Broede B, Thomsen M, Pfeiffer V, Wörsdörfer P, Karnati S, Wagner N, Rueckschloss U, Ergün S. Aging-related carcinoembryonic antigen-related cell adhesion molecule 1 signaling promotes vascular dysfunction. *Aging Cell*. 2019; 18:e13025.  
<https://doi.org/10.1111/acer.13025>  
PMID:[31389127](https://pubmed.ncbi.nlm.nih.gov/31389127/)
  30. Zou Y, Yoon S, Jung KJ, Kim CH, Son TG, Kim MS, Kim YJ, Lee J, Yu BP, Chung HY. Upregulation of aortic adhesion molecules during aging. *J Gerontol A Biol Sci Med Sci*. 2006; 61:232–44.  
<https://doi.org/10.1093/gerona/61.3.232>  
PMID:[16567371](https://pubmed.ncbi.nlm.nih.gov/16567371/)
  31. Dincer S. Collection of hemopoietic stem cells in

- allogeneic female donors during menstrual bleeding. *Transfus Apher Sci.* 2004; 30:175–6.  
<https://doi.org/10.1016/j.transci.2003.12.001>  
PMID:15062759
32. Skaznik-Wikiel ME, McGuire MM, Sukhwani M, Donohue J, Chu T, Krivak TC, Rajkovic A, Orwig KE. Granulocyte colony-stimulating factor with or without stem cell factor extends time to premature ovarian insufficiency in female mice treated with alkylating chemotherapy. *Fertil Steril.* 2013; 99:2045–54.e3.  
<https://doi.org/10.1016/j.fertnstert.2013.01.135>  
PMID:23453120
33. Akdemir A, Zeybek B, Akman L, Ergenoglu AM, Yeniel AO, Erbas O, Yavasoglu A, Terek MC, Taskiran D. Granulocyte-colony stimulating factor decreases the extent of ovarian damage caused by cisplatin in an experimental rat model. *J Gynecol Oncol.* 2014; 25:328–33.  
<https://doi.org/10.3802/jgo.2014.25.4.328>  
PMID:25142624
34. Lee D, Jo JD, Kim SK, Jee BC, Kim SH. The efficacy of intrauterine instillation of granulocyte colony-stimulating factor in infertile women with a thin endometrium: A pilot study. *Clin Exp Reprod Med.* 2016; 43:240–6.  
<https://doi.org/10.5653/cerm.2016.43.4.240>  
PMID:28090464
35. Eftekhari M, Sayadi M, Arabjahvani F. Transvaginal perfusion of G-CSF for infertile women with thin endometrium in frozen ET program: A non-randomized clinical trial. *Iran J Reprod Med.* 2014; 12:661–6.  
PMID:25469123
36. Sasaki H, Hamatani T, Kamijo S, Iwai M, Kobanawa M, Ogawa S, Miyado K, Tanaka M. Impact of Oxidative Stress on Age-Associated Decline in Oocyte Developmental Competence. *Front Endocrinol (Lausanne).* 2019; 10:811.  
<https://doi.org/10.3389/fendo.2019.00811>  
PMID:31824426
37. Devesa J, Caicedo D. The Role of Growth Hormone on Ovarian Functioning and Ovarian Angiogenesis. *Front Endocrinol (Lausanne).* 2019; 10:450.  
<https://doi.org/10.3389/fendo.2019.00450>  
PMID:31379735
38. Mauro A, Martelli A, Berardinelli P, Russo V, Bernabò N, Di Giacinto O, Mattioli M, Barboni B. Effect of antiprogestosterone RU486 on VEGF expression and blood vessel remodeling on ovarian follicles before ovulation. *PLoS One.* 2014; 9:e95910.  
<https://doi.org/10.1371/journal.pone.0095910>  
PMID:24756033
39. Tan XM, Zhang XL, Ji MM, Yu KL, Liu MM, Tao YC, Yu ZL. Differentially expressed genes associated with primordial follicle formation and transformation to primary Follicles. *Reprod Dev Med.* 2018; 2:142–9.  
<http://dx.doi.org/10.4103/2096-2924.248484>.
40. Gougeon A. Human ovarian follicular development: from activation of resting follicles to preovulatory maturation. *Ann Endocrinol (Paris).* 2010; 71:132–43.  
<https://doi.org/10.1016/j.ando.2010.02.021>  
PMID:20362973
41. Muhammad T, Wan Y, Sha Q, Wang J, Huang T, Cao Y, Li M, Yu X, Yin Y, Chan WY, Chen ZJ, You L, Lu G, Liu H. IGF2 improves the developmental competency and meiotic structure of oocytes from aged mice. *Aging (Albany NY).* 2020; 13:2118–34.  
<https://doi.org/10.18632/aging.202214>  
PMID:33318299
42. Wan Y, Muhammad T, Huang T, Lv Y, Sha Q, Yang S, Lu G, Chan WY, Ma J, Liu H. IGF2 reduces meiotic defects in oocytes from obese mice and improves embryonic developmental competency. *Reprod Biol Endocrinol.* 2022; 20:101.  
<https://doi.org/10.1186/s12958-022-00972-9>  
PMID:35836183
43. Ambekar AS, Kelkar DS, Pinto SM, Sharma R, Hinduja I, Zaveri K, Pandey A, Prasad TS, Gowda H, Mukherjee S. Proteomics of follicular fluid from women with polycystic ovary syndrome suggests molecular defects in follicular development. *J Clin Endocrinol Metab.* 2015; 100:744–53.  
<https://doi.org/10.1210/jc.2014-2086>  
PMID:25393639
44. Devarbhavi P, Telang L, Vastrad B, Tengli A, Vastrad C, Kotturshetti I. Identification of key pathways and genes in polycystic ovary syndrome via integrated bioinformatics analysis and prediction of small therapeutic molecules. *Reprod Biol Endocrinol.* 2021; 19:31.  
<https://doi.org/10.1186/s12958-021-00706-3>  
PMID:33622336
45. Wilcox SM, Arora H, Munro L, Xin J, Fenninger F, Johnson LA, Pfeifer CG, Choi KB, Hou J, Hoodless PA, Jefferies WA. The role of the innate immune response regulatory gene ABCF1 in mammalian embryogenesis and development. *PLoS One.* 2017; 12:e0175918.  
<https://doi.org/10.1371/journal.pone.0175918>  
PMID:28542262
46. R Core Team. R: A language and environment for statistical computing. R Foundation for Statistical Computing, Vienna, Austria. 2015. <https://www.R-project.org/>.

## SUPPLEMENTARY MATERIALS

### Supplementary Methods

#### **Library construction: sample pool protein extraction, digestion and LC-MS/MS SWATH™**

A sample pool was generated by combining 15 µL aliquots from each patient samples. Of this sample pool, 50 µL was precipitated with ice-cold ethanol at a final concentration of 40% during 2 h at 5°C. The sample was then centrifuged for 1 h at 15,000 g and the supernatant (containing human serum albumin (HSA)) was removed. The pellet was left to air dry and the precipitated proteins were validated using 1:1 dilution in 150 nM NaCl loaded onto a 12% SDS-PAGE gel stained with Coomassie Colloidal. To reduce the protein complexity for the LC-MS/MS analysis, the gel was fractionated into slices and incubated overnight at 37°C with 500 ng sequencing grade trypsin (Promega, WI, USA) for enzymatic digestion, as previously described (12). The digestion was stopped with 20% trifluoroacetic acid and the supernatant was removed before dehydrating the library gel slides with pure acetonitrile. The new peptide solutions were combined with the corresponding supernatant, dried in a speed vacuum and resuspended in 2% acetonitrile, 0.1% trifluoroacetic acid. The final volume was adjusted (from 6–10 µL) according to the intensity of the staining.

LC-MS/MS was adapted from a previously described protocol (13) set up in similar samples. Digested peptide mixtures (5 µL) were loaded onto NanoLC Columns (3 µ C18-CL, 75 µm × 15 cm; Eksigent Technologies, CA, USA) and desalted with 0.1% trifluoroacetic acid at 3 µl/min during 5 mins. Analytical columns (LC Column, 3 µ C18-CL, 75 µm × 12 cm; Nikkyo, Japan) were equilibrated in acetonitrile solution (5% acetonitrile with 0.1% formic acid) before eluting peptides with a linear gradient of 5–35% acetonitrile solution in 0.1% formic acid for 30 min at a flow rate of 300 nL/min. Peptides were analyzed in a mass spectrometer nanoESI qTOF (5600 TripleTOF; ABSCIEX, MA, USA) and a library was created by combining all the data. ProteinPilot (v.5.0) default parameters were used to generate a peak list directly from 5600 TripleTof wiff files. The Paragon algorithm

(14) was used to search the Swissprot database (03.2018) with the following parameters: trypsin specificity, cys-alkylation, without taxonomy restriction, and the search effort set to through and false discovery rate (FDR) correction for proteins. To avoid using the same spectral evidence in more than one protein, the identified proteins were grouped based on MS/MS spectra by the ProteinPilot Progroup algorithm. Furthermore, data obtained in this experiment was combined with all the data of human plasma generated in the proteomic laboratory of the Central Service for Experimental Research (SCSIE; University of Valencia), to create a Pan Serum Spectrum Library, and amplify the number of proteins represented in the library from 337 to 507.

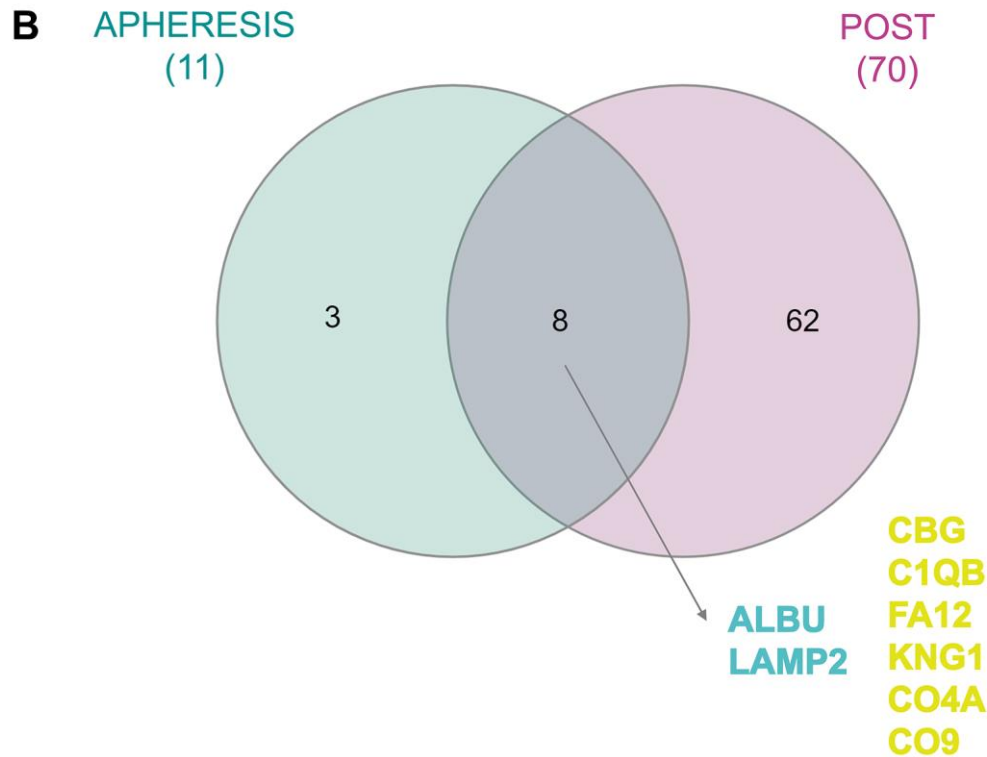
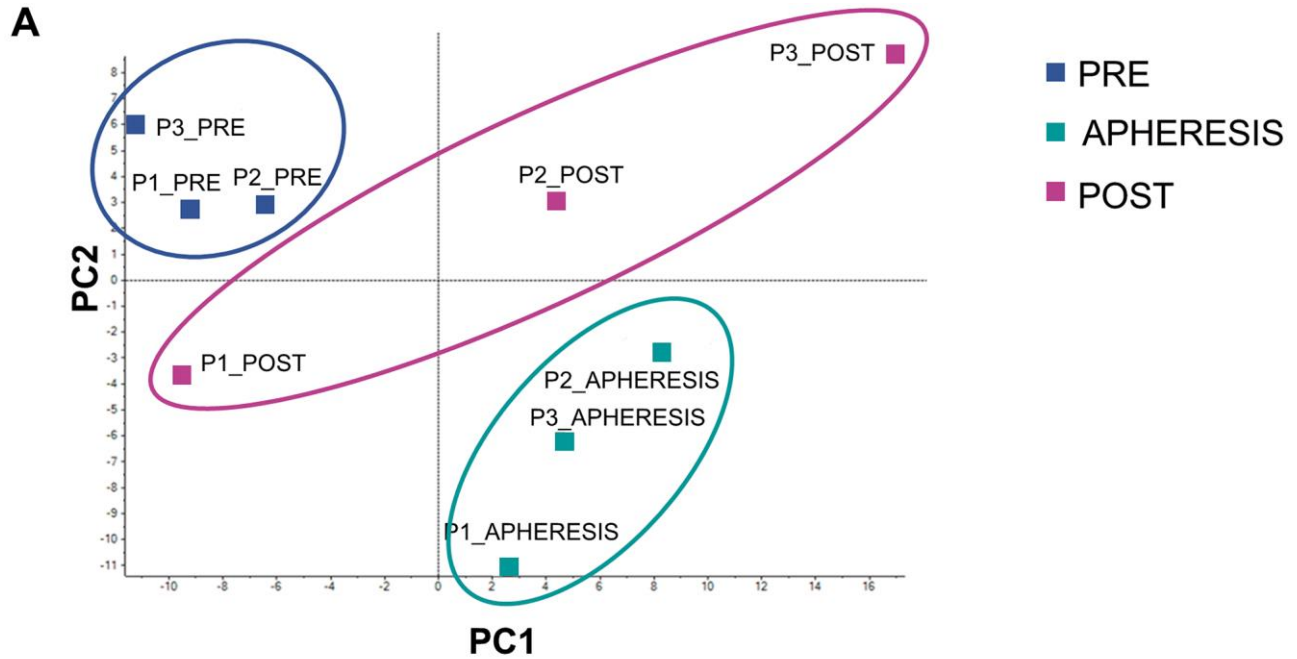
#### **Individual sample protein extraction, quantification and digestion**

One hundred µL of each individual plasma sample was delipidated by centrifugation and 85 µL of delipidated plasma was precipitated with ethanol 40% to remove HSA as explained above. The pellets were dissolved with 100 µL of 0.5 M Tetraethylammonium bromide with 4 M Urea and 2% SDS and the final solutions were quantified with a protein quantification assay (Machery-Nagel, France) according the manufacturer protocol. Samples (25 µg) were then loaded without resolving in 1D PAGE gels and incubated overnight at 37°C with 500 ng sequencing grade trypsin (Promega, WI, USA) for enzymatic digestion, as previously described (12). The digestion was stopped with 20% trifluoroacetic acid and the supernatant was removed before dehydrating the gels with pure acetonitrile. The peptide solutions were dried in a vacuum centrifuge and resuspended in 50 µL 2% acetonitrile, 0.1% trifluoroacetic acid.

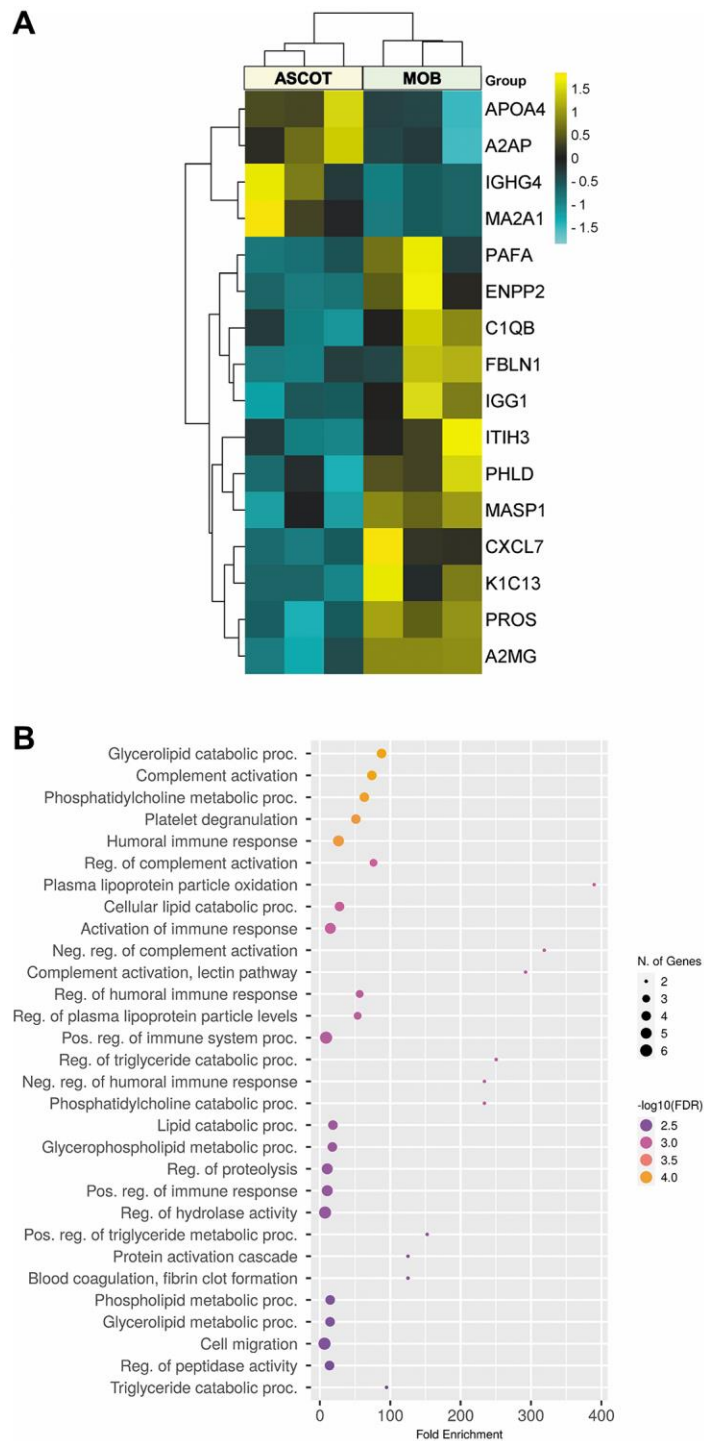
#### **Processing settings used for peptide selection in individual samples**

The following processing settings were applied to select peptides in the nine individual plasma samples: 20 peptides/protein, 6 transitions/peptide, 95% peptide confidence threshold, 1% FDR, exclude modified peptides. XIC options were set to 20 min XIC extraction windows and 50 ppm for XIC width.

Supplementary Figures



**Supplementary Figure 1. Differences and similarities between immediate and lasting proteomic changes induced by stem cell mobilization and injection in women with poor ovarian response (POR).** (A) Principal component analysis plot considering the expression of the 296 quantified proteins, showing a clear separation between PRE, APHERESIS and POST samples. (B) Venn diagram highlighting the share differentially expressed proteins between APHERESIS vs. PRE and POST vs. PRE comparisons.



**Supplementary Figure 2. Comparison of the proteomic effects induced by stem cell mobilization, *per se*, and by stem cell injection three months after the procedures in women with premature ovarian insufficiency (POI). (A) Heatmap depicting the hierarchical clustering of the 16 differentially expressed proteins between POST samples of both study arms: mobilization (MOB) and autologous stem cell ovarian transplantation (ASCOT). (B) Dot plot showing the corresponding top 30 significantly enriched (FDR < 0.05) GO biological processes.**

## Supplementary Tables

Please browse Full Text version to see the data of Supplementary Tables 1 and 6.

**Supplementary Table 1. Proteomic profile of plasma before (PRE), during (APHERESIS) and after (POST) stem cell mobilization and infusion in women with poor ovarian response (POR).**

**Supplementary Table 2. Differentially expressed proteins between PRE and APHERESIS samples in women with poor ovarian response (POR).**

Protein ID	Protein name	Protein abbreviation name	Gene name	Estimate
P02750	Leucine-rich alpha-2-glycoprotein	A2GL	LRG1	1,771
P01042	Kininogen-1	KNG1	KNG1	1,638
P02746	Complement C1q subcomponent subunit B	C1QB	C1QB	1,562
P10909	Clusterin	CLUS	CLU	1,299
P02748	Complement component C9	CO9	C9	1,053
P08185	Corticosteroid-binding globulin	CBG	SERPINA6	0,983
P06727	Apolipoprotein A-IV	APOA4	APOA4	0,953
P0C0L4	Complement C4-A	CO4A	C4A	0,727
P00748	Coagulation factor XII	FA12	F12	0,664
P02768	Serum albumin	ALBU	ALB	-0,414
P13473	Lysosome-associated membrane glycoprotein 2	LAMP2	LAMP2	-1,362

**Supplementary Table 3. Differentially expressed proteins between POST and APHERESIS samples in women with poor ovarian response (POR).**

Protein ID	Protein name	Protein abbreviation name	Gene name	Estimate
Q8TER0	Sushi, nidogen and EGF-like domain-containing protein 1	SNED1	SNED1	2,335
P13796	Plastin-2	PLSL	LCP1	2,164
P19320	Vascular cell adhesion protein 1	VCAM1	VCAM1	2,133
P11597	Cholesteryl ester transfer protein	CETP	CETP	1,863
P18428	Lipopolysaccharide-binding protein	LBP	LBP	1,788
P14543	Nidogen-1	NID1	NID1	1,709
P08571	Monocyte differentiation antigen CD14	CD14	CD14	1,647
P02679	Fibrinogen gamma chain	FIBG	FGG	1,624
P0DOX8	Immunoglobulin lambda-1 light chain	IGL1	IGL1	1,624
O00533	Neural cell adhesion molecule L1-like protein	NCHL1	CHL1	1,623
P00751	Complement factor B	CFAB	CFB	1,615
P19827	Inter-alpha-trypsin inhibitor heavy chain H1	ITIH1	ITIH1	1,551
P04275	von Willebrand factor	VWF	VWF	1,505
P07360	Complement component C8 gamma chain	CO8G	C8G	1,455
P10643	Complement component C7	CO7	C7	1,439
P00488	Coagulation factor XIII A chain	F13A	F13A1	1,437
P02746	Complement C1q subcomponent subunit B	C1QB	C1QB	1,404
P12259	Coagulation factor V	FA5	F5	1,390
P19823	Inter-alpha-trypsin inhibitor heavy chain H2	ITIH2	ITIH2	1,379
P05546	Heparin cofactor 2	HEP2	SERPIND1	1,376

<b>P01011</b>	Alpha-1-antichymotrypsin	AACT	SERPINA3	1,293
<b>P00748</b>	Coagulation factor XII	FA12	F12	1,243
<b>P29622</b>	Kallistatin	KAIN	SERPINA4	1,234
<b>P06396</b>	Gelsolin	GELS	GSN	1,231
<b>P09871</b>	Complement C1s subcomponent	C1S	C1S	1,217
<b>Q12805</b>	EGF-containing fibulin-like extracellular matrix protein 1	FBLN3	EFEMP1	1,207
<b>P0COL4</b>	Complement C4-A	CO4A	C4A	1,198
<b>P02748</b>	Complement component C9	CO9	C9	1,186
<b>P05156</b>	Complement factor I	CFAI	CFI	1,145
<b>P23142</b>	Fibulin-1	FBLN1	FBLN1	1,114
<b>P07225</b>	Vitamin K-dependent protein S	PROS	PROS1	1,106
<b>P09211</b>	Glutathione S-transferase P	GSTP1	GSTP1	1,104
<b>P00740</b>	Coagulation factor IX	FA9	F9	1,098
<b>P15169</b>	Carboxypeptidase N catalytic chain	CBPN	CPN1	1,058
<b>P14151</b>	L-selectin	LYAM1	SELL	1,051
<b>P80748</b>	Immunoglobulin lambda variable 3-21	LV321	IGLV3-21	1,015
<b>P02675</b>	Fibrinogen beta chain	FIBB	FGB	1,002
<b>P05543</b>	Thyroxine-binding globulin	THBG	SERPINA7	0,990
<b>Q06033</b>	Inter-alpha-trypsin inhibitor heavy chain H3	ITIH3	ITIH3	0,971
<b>P36955</b>	Pigment epithelium-derived factor	PEDF	SERPINF1	0,944
<b>Q9BXR6</b>	Complement factor H-related protein 5	FHR5	CFHR5	0,934
<b>P01042</b>	Kininogen-1	KNG1	KNG1	0,930
<b>P43251</b>	Biotinidase	BTD	BTD	0,903
<b>P55058</b>	Phospholipid transfer protein	PLTP	PLTP	0,873
<b>P08185</b>	Corticosteroid-binding globulin	CBG	SERPINA6	0,835
<b>Q9UK55</b>	Protein Z-dependent protease inhibitor	ZPI	SERPINA10	0,815
<b>P22792</b>	Carboxypeptidase N subunit 2	CPN2	CPN2	0,794
<b>Q96KN2</b>	Beta-Ala-His dipeptidase	CNDP1	CNDP1	0,785
<b>Q14624</b>	Inter-alpha-trypsin inhibitor heavy chain H4	ITIH4	ITIH4	0,784
<b>Q9P225</b>	Dynein heavy chain 2, axonemal	DYH2	DNAH2	0,755
<b>P05155</b>	Plasma protease C1 inhibitor	IC1	SERPING1	0,751
<b>P01703</b>	Immunoglobulin lambda variable 1-40	LV140	IGLV1-40	0,720
<b>A0A0C4DH38</b>	Immunoglobulin heavy variable 5-51	HV551	IGHV5-51	0,719
<b>P01009</b>	Alpha-1-antitrypsin	A1AT	SERPINA1	0,716
<b>P06276</b>	Cholinesterase	CHLE	BCHE	0,712
<b>P01008</b>	Antithrombin-III	ANT3	SERPINC1	0,623
<b>O14791</b>	Apolipoprotein L1	APOL1	APOL1	0,616
<b>P08697</b>	Alpha-2-antiplasmin	A2AP	SERPINF2	0,602
<b>Q92820</b>	Gamma-glutamyl hydrolase	GGH	GGH	0,584
<b>Q9Y6R7</b>	IgGfc-binding protein	FCGBP	FCGBP	0,534
<b>P01624</b>	Immunoglobulin kappa variable 3-15	KV315	IGKV3-15	0,415
<b>P12035</b>	Keratin, type II cytoskeletal 3	K2C3	KRT3	-0,383
<b>P02768</b>	Serum albumin	ALBU	ALB	-0,543
<b>P43652</b>	Afamin	AFAM	AFM	-0,613
<b>P02656</b>	Apolipoprotein C-III	APOC3	APOC3	-0,884
<b>P02774</b>	Vitamin D-binding protein	VTDB	GC	-0,932
<b>Q13103</b>	Secreted phosphoprotein 24	SPP24	SPP2	-0,948
<b>P13473</b>	Lysosome-associated membrane glycoprotein 2	LAMP2	LAMP2	-1,163

<b>P32119</b>	Peroxiredoxin-2	PRDX2	PRDX2	-2,298
<b>P69905</b>	Hemoglobin subunit alpha	HBA	HBA1	-3,616

The most prominent changes after ASCOT, considering the estimated fold change, are highlighted in yellow (upregulations) or blue (downregulations).

**Supplementary Table 4. Ovarian reserve biomarkers of women with premature ovarian insufficiency (POI) before autologous stem cell ovarian transplantation (ASCOT) and three months after this reactivation technique.**

Parameter	All (n = 6)		ASCOT arm (n = 3)		Mobilization arm (n = 3)	
	PRE	POST	PRE	POST	PRE	POST
<b>AMH (pmol/L)</b>	0.1 ± 0.1	0.3 ± 0.3*	0.1 ± 0.0	0.4 ± 0.3	0.1 ± 0.1	0.2 ± 0.1
<b>AFC (n)</b>	1.5 ± 1.2	2.5 ± 2.6	1.3 ± 0.9	2.0 ± 2.0	1.7 ± 1.5	3.0 ± 2.8
<b>FSH (IU/mL)</b>	99.9 ± 23.9	54.9 ± 35.9*	100.3 ± 17.3	60.2 ± 38.2*	99.5 ± 31.2	49.6 ± 33.6*

Wilcoxon nonparametric paired test was applied to compare PRE and POST ovarian reserve biomarkers for each patient, indicating the asterisk a *p*-value < 0.05. Abbreviations: AMH: anti-müllerian hormone; AFC: antral follicular count; FSH: follicle-stimulating hormone.

**Supplementary Table 5. Protocols of controlled ovarian stimulation (COS) performed in patients with premature ovarian insufficiency (POI) after autologous stem cell ovarian transplantation (ASCOT) technique.**

Parameter	All (n = 6)	ASCOT arm (n = 3)	Mobilization arm (n = 3)
<b>COS cycles (n total)</b>	11	5	6
<b>FSH (IU/mL)</b>	39.7 ± 16.8	38.1 ± 13.4	41.0 ± 20.4
<b>AMH (pM)</b>	0.4 ± 0.6	0.7 ± 0.8	0.1 ± 0.1
<b>Days of stimulation</b>	8.6 ± 5.8	5.4 ± 5.9	11.3 ± 4.6
<b>E2 hCG day</b>	189.2 ± 182.5	276.5 ± 222.2	116.3 ± 114.7
<b>AFC total</b>	1.6 ± 0.9	1.8 ± 1.1	1.5 ± 0.8
<b>Punctured follicles</b>	0.8 ± 0.4	1.0 ± 0.0	0.7 ± 0.5
<b>MII oocytes</b>	0.3 ± 0.5	0.4 ± 0.6	0.2 ± 0.4
<b>Embryos</b>	0.3 ± 0.5	0.3 ± 0.5	0.3 ± 0.5
<b>Cancellation</b>	2/11 (18.2%)	0/5 (0%)	2/6 (33.3%)

**Supplementary Table 6. Proteomic profile of plasma before (PRE), during (APHERESIS) and after (POST) stem cell mobilization and infusion in women with premature ovarian insufficiency (POI).**

**Supplementary Table 7. Differentially expressed proteins between all PRE and APHERESIS samples in women with premature ovarian insufficiency (POI).**

Protein ID	Protein name	Protein abbreviation name	Gene name	Estimate
<b>P02745</b>	Complement C1q subcomponent subunit A	C1QA	C1QA	2,75
<b>P00736</b>	Complement C1r subcomponent	C1R	C1R	2,70
<b>P14151</b>	L-selectin	LYAM1	SELL	1,45
<b>P59666</b>	Neutrophil defensin 3	DEF3	DEFA3	0,81
<b>P00740</b>	Coagulation factor IX	FA9	F9	0,65
<b>P08571</b>	Monocyte differentiation antigen CD14	CD14	CD14	0,51
<b>P02748</b>	Complement component C9	CO9	C9	0,51
<b>P61626</b>	Lysozyme C	LYSC	LYZ	0,43

<b>P02747</b>	Complement C1q subcomponent subunit C	C1QC	C1QC	0,35
<b>P21333</b>	Filamin-A	FLNA	FLNA	0,25
<b>P0DOX5</b>	Immunoglobulin gamma-1 heavy chain	IGG1	1 SV	0,22
<b>P02741</b>	C-reactive protein	CRP	CRP	-0,21
<b>P32754</b>	4-hydroxyphenylpyruvate dioxygenase	HPPD	HPD	-0,28
<b>P11362</b>	Fibroblast growth factor receptor 1	FGFR1	FGFR1	-0,43

**Supplementary Table 8. Differentially expressed proteins between PRE and POST samples in the mobilization arm.**

<b>Protein ID</b>	<b>Protein name</b>	<b>Protein abbreviation name</b>	<b>Gene name</b>	<b>Estimate</b>
<b>P01344</b>	Insulin-like growth factor II	IGF2	IGF2	0,66
<b>P05109</b>	Protein S100-A8	S10A8	S100A8	0,51
<b>Q15582</b>	Transforming growth factor-beta-induced protein ig-h3	BGH3	TGFBI	0,45
<b>P05451</b>	Lithostathine-1-alpha	REG1A	REG1A	0,30
<b>Q8IX21</b>	SMC5-SMC6 complex localization factor protein 2	SLF2	SLF2	0,27
<b>P02776</b>	Platelet factor 4	PLF4	PF4	0,25
<b>P15924</b>	Desmoplakin	DESP	DSP	0,25
<b>P01861</b>	Immunoglobulin heavy constant gamma 4	IGHG4	IGHG4	0,24
<b>O43866</b>	CD5 antigen-like	CD5L	CD5L	0,15
<b>P07996</b>	Thrombospondin-1	TSP1	THBS1	0,14
<b>P08253</b>	72 kDa type IV collagenase	MMP2	MMP2	0,12
<b>P33908</b>	Mannosyl-oligosaccharide 1,2-alpha-mannosidase IA	MA1A1	MAN1A1	0,12
<b>P00966</b>	Argininosuccinate synthase	ASSY	ASS1	0,11
<b>P02671</b>	Fibrinogen alpha chain	FIBA	FGA	0,10
<b>P08709</b>	Coagulation factor VII	FA7	F7	0,06
<b>P0DML3</b>	Chorionic somatomammotropin hormone 2	CSH2	CSH2	0,05
<b>P00450</b>	Ceruloplasmin	CERU	CP	0,04
<b>P09972</b>	Fructose-bisphosphate aldolase C	ALDOC	ALDOC	0,02
<b>P11226</b>	Mannose-binding protein C	MBL2	MBL2	-0,01
<b>P11021</b>	Endoplasmic reticulum chaperone BiP	BIP	HSPA5	-0,01
<b>P04003</b>	C4b-binding protein alpha chain	C4BPA	C4BPA	-0,08
<b>Q12860</b>	Contactin-1	CNTN1	CNTN1	-0,20
<b>O75882</b>	Attractin	ATRN	ATRN	-0,24
<b>P33151</b>	Cadherin-5	CADH5	CDH5	-0,54

**Supplementary Table 9. Differentially expressed proteins between PRE and POST samples in the ASCOT arm. Table supplied in excel format.**

<b>Protein ID</b>	<b>Protein name</b>	<b>Protein abbreviation name</b>	<b>Gene name</b>	<b>Estimate</b>
<b>P61769</b>	Beta-2-microglobulin	B2MG	B2M	0,35
<b>P01344</b>	Insulin-like growth factor II	IGF2	IGF2	0,23
<b>Q01459</b>	Di-N-acetylchitobiase	DIAC	CTBS	-0,02
<b>P31944</b>	Caspase-14	CASPE	CASP14	-0,33
<b>Q7Z7G0</b>	Target of Nesh-SH3	TARSH	ABI3BP	-0,35
<b>Q8NE71</b>	ATP-binding cassette sub-family F member 1	ABCF1	ABCF1	-0,43
<b>P06396</b>	Gelsolin	GELS	GSN	-0,49

<b>P43251</b>	Biotinidase	BTD	BTD	-0,50
<b>O00299</b>	Chloride intracellular channel protein 1	CLIC1	CLIC1	-0,52
<b>P05160</b>	Coagulation factor XIII B chain	F13B	F13B	-0,61
<b>P01031</b>	Complement C5	CO5	C5	-2,97

**Supplementary Table 10. Differentially expressed proteins between POST samples of both arms of the study (mobilization and ASCOT). Table supplied in excel format.**

<b>Protein ID</b>	<b>Protein name</b>	<b>Protein abbreviation name</b>	<b>Gene name</b>	<b>Estimate</b>
<b>P06727</b>	Apolipoprotein A-IV	APOA4	APOA4	0,64
<b>P08697</b>	Alpha-2-antiplasmin	A2AP	SERPINF2	0,56
<b>Q16706</b>	Alpha-mannosidase 2	MA2A1	MAN2A1	0,49
<b>P01861</b>	Immunoglobulin heavy constant gamma 4	IGHG4	IGHG4	0,22
<b>P23142</b>	Fibulin-1	FBLN1	FBLN1	0,00
<b>Q13093</b>	Platelet-activating factor acetylhydrolase	PAFA	PLA2G7	-0,39
<b>Q06033</b>	Inter-alpha-trypsin inhibitor heavy chain H3	ITIH3	ITIH3	-0,48
<b>P0DOX5</b>	Immunoglobulin gamma-1 heavy chain	IGG1	1 SV	-0,65
<b>P02775</b>	Platelet basic protein	CXCL7	PPBP	-0,66
<b>P13646</b>	Keratin, type I cytoskeletal 13	K1C13	KRT13	-0,88
<b>P02746</b>	Complement C1q subcomponent subunit B	C1QB	C1QB	-1,04
<b>Q13822</b>	Ectonucleotide pyrophosphatase/phosphodiesterase family member 2	ENPP2	ENPP2	-1,69
<b>P07225</b>	Vitamin K-dependent protein S	PROS	PROS1	-1,95
<b>P01023</b>	Alpha-2-macroglobulin	A2MG	A2M	-2,11
<b>P80108</b>	Phosphatidylinositol-glycan-specific phospholipase D	PHLD	GPLD1	-2,60
<b>P48740</b>	Mannan-binding lectin serine protease 1	MASP1	MASP1	-3,84